

Cite this: *New J. Chem.*, 2012, **36**, 1170–1179

www.rsc.org/njc

PAPER

Tripod facial surfactants with benzene as the central core: design, synthesis and self-assembly study†

Julien Dauvergne,^{ab} Anissa Bendjeriou,^{ab} Françoise Bonneté,^{ab}
Joachim Kohlbrecher,^c Bernard Pucci,^{ab} Laurie-Anne Barret^{ab} and Ange Polidori^{*ab}

Received (in Montpellier, France) 11th October 2011, Accepted 15th February 2012

DOI: 10.1039/c2nj20876h

The design, synthesis and self-assembled study of a new class of benzene-derived tripod facial amphiphiles are reported. The synthetic route chosen based on a central mesitylene as scaffold allows easy tuning of lipophilic and hydrophilic groups and thus control of the tensioactive properties of these new surfactants. This new class of surfactants exhibits three glucose moieties as the hydrophilic polar head and three hydrocarbon chains each having 3 to 7 carbons as the lipophilic part. These tripod facial amphiphiles exhibit well-defined tensioactive and aggregative properties. Their critical aggregation concentration, their particle size in water (less than 20 nm), and their aggregation behavior are closely linked to the nature of their lipophilic chains and can therefore be easily modulated.

Introduction

In the last few decades, synthetic amphiphiles with unusual architectures such as bolaamphiphiles or gemini surfactants have been obtained.¹ Amphiphilic surfactants too, sometimes called facial or contrafacial surfactants, have attracted increasing interest.² They are defined as molecules with a rigid framework (such as the steroid skeleton) with hydrophilic and lipophilic parts located on two opposite faces.^{3,4} The controlled self-assembly of facial amphiphiles offers an attractive opportunity to construct defined aggregates and supramolecular architectures, specifically designed for particular applications. Currently, cholic acid is the most popular platform for the design of facial amphiphiles, leading researchers to derivatize its hydroxyl groups by grafting on sugars, carboxylates, amines/ammoniums and sulfonates, thus enhancing its facial amphiphilic character.^{5–10a} Non-steroidal facial amphiphiles have also been synthesized with a block pattern derived from bridged annulene^{10b} or [2 + 2] and [4 + 2] norbornadiene cycloaddition cores.¹¹ In recent years, other facial amphiphiles with original scaffolds have appeared in the literature.

For example, clip-like glycoluril-based structures display an interesting counterion-dependent aggregation.¹² Amphiphilic calix[4]arene scaffolds possessing lipophilic side chains on the lower rim and either dendritic hydrophilic residues or carboxylic moieties on the upper rim have also been obtained.^{13–15} Kellermann *et al.*¹⁴ showed that these amphiphiles adopt a cone-shaped conformation involving small aggregates of high curvature, forming uniform aggregates consisting of seven units, non-deformable upon drying. Facially amphiphilic dendrimers have also been designed, forming well-controlled and stable self-assembled structures.^{16–18} Facial amphiphiles offer particular promise in biology, where they can be used to overcome difficulties in handling membrane proteins in aqueous solution.¹⁰

Here, we describe how we designed the synthesis of a new class of benzene-based tripod facial amphiphiles and determined their tensioactive and aggregative properties in aqueous media. These new facial amphiphiles were prepared following a chemical pathway based on a central benzene group as scaffold (Fig. 1).

Simple chemical modifications of this aromatic core allow lipophilic and hydrophilic moieties to be tuned easily. Regarding the aromatic ring, persubstituted aromatic compounds having a D_{3d} symmetry structure have been shown to adopt an alternating up–down conformational network in which cooperative interactions direct the vicinal groups to point to opposite sides of the benzene ring, resulting in a 1,3,5/2,4,6 facial segregation.¹⁹ In the present case, the lipophilic face of these amphiphiles is made up of three short hydrocarbon chains each having 3 to 7 carbons and the hydrophilic face consists of 3 glucosyl groups introduced *via* click-chemistry resources. The physico-chemical properties of these facial

^a Université d'Avignon et des Pays de Vaucluse, Faculté des Sciences, Équipe Chimie Bioorganique et Systèmes Amphiphiles, 33, rue Louis Pasteur, 84000 Avignon, France.

E-mail: ange.polidori@univ-avignon.fr

^b Institut des Biomolécules Max Mousseron, UMR 5247, CNRS—Universités Montpellier I et II 15, avenue Charles Flahault, 34093 Montpellier cedex 05, France

^c Laboratory for Neutron Scattering, Paul Scherrer Institut, 5232 Villigen PSI, Switzerland

† Electronic supplementary information (ESI) available: TEM micrographs of a dispersion of **C7Glu3** in water after sonication, all ¹H and ¹³C NMR spectra scanned of tripod compounds **CnGlu3** and some data concerning SAXS experiments. See DOI: 10.1039/c2nj20876h

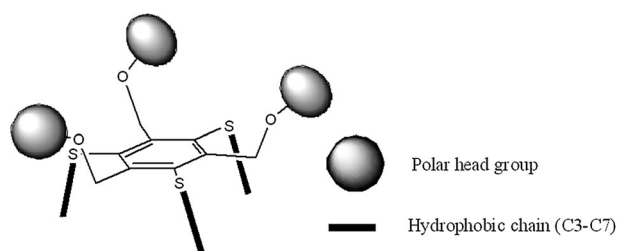


Fig. 1 General structure of tripod amphiphiles with 1,3,5/2,4,6 facial segregation.¹⁹

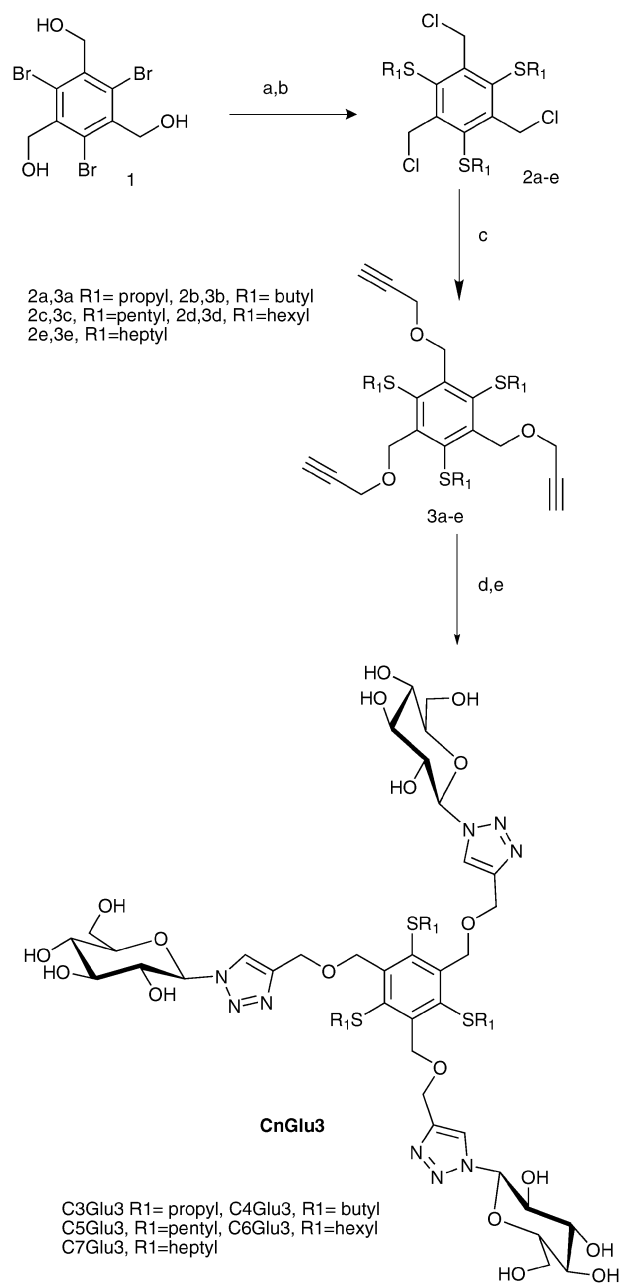
amphiphiles, notably tensioactive properties, shape and size of aggregates, are closely linked to the length of the lipophilic chains grafted onto the benzene ring.

Results and discussion

The key step in obtaining alternately substituted benzene was the sequential functionalization of 1,3,5-tribromo-2,4,6-trihydroxymethyl-benzene **1**, which can easily be achieved on a multiple-gram scale. Its synthesis from mesitylene as starting material, as described by Anthony *et al.*,²⁰ involves a four-step synthetic route giving a 59% overall yield. In the present case we obtained a 90 g batch without chromatography, which we used to synthesize tripod facial amphiphiles according to the chemical route depicted in Scheme 1.

The first decisive step involved a threefold nucleophilic aromatic substitution of **1** by thiolate anions derived from either propyl (a), butyl (b), pentyl (c), hexyl (d) or heptyl mercaptan (e). The reaction proceeded smoothly under mild conditions to give thioether compounds in excellent yield, due to the use of 1,3-dimethyl-2-imidazolidone (DMI) as solvent rather than DMF, which requires harsher conditions.²¹ To efficiently introduce the three hydrophilic groups onto the aromatic core, copper(i)-catalyzed alkyne-azide cycloaddition was used. The hydroxyl groups were subjected to mesylation using a combination of methanesulfonyl chloride/TEA in cold CH₂Cl₂. Surprisingly, the reaction afforded the trichlorinated derivatives **2a–e** instead of the desired products. The mesylate groups produced in the reaction mixture appear to be substituted again by the existing chloride ions. Conversion requires a long reaction time but the product is formed in high yields with good purity.

The subsequent substitution of chlorine groups by propargyl alcoholate in DMF readily provided the trisubstituted derivatives **3a–e** in 60% yield. The addition of 1-azido-1-deoxy-β-D-glucopyranoside tetraacetate on trisubstituted derivatives **3a–e** in the presence of active CuI as catalyst afforded triglucosylated compounds in good yield after 24 h reaction time at room temperature. Finally, deprotection of acetyl groups by transesterification in the presence of sodium methoxide as catalyst provided tripod facial amphiphiles (**CnGlu3**). These alkyne derivatives **3a–e** were used to efficiently attach sugar moieties by the usual Cu(i)-catalyzed azide-alkyne [1,3]-dipolar cycloaddition reaction, in high yield and with complete regioselectivity according to the optimized procedure for glycolipid analogues.^{22,23} The treatment of derivatives **3a–e** and peracetylated glucosylazide in THF by direct use of active CuI(i) as catalyst



Scheme 1 Synthetic route leading to tripod facial amphiphiles **CnGlu3**, reagents, temperature, time and yield: (a) R₁SH, tBuOK, DMI, rt, 16 h, 97%; (b) Et₃N, MsCl, CH₂Cl₂, 5 °C → rt., 48 h, 83%; (c) propargyl alcohol, NaH 60%, THF/DMF (1 : 1), 0 °C → rt., 18 h, 65%; (d) 1-azido-1-deoxy-β-D-glucopyranoside tetraacetate, DIEA, CuI, THF, rt, 24 h, 71%; (e) MeONa cat., MeOH/THF (4 : 1), pH 9–10, rt, 24 h, 93%.

combined with DIEA, after a 24 h reaction time to ensure complete conversion, afforded stereoselective acetylated compounds **CnGlu3** in good yield. This was confirmed by ¹H NMR spectra, which revealed a characteristic peak at around 8 ppm assigned to the triazole protons and disappearance of the triplet at around 2.5 ppm assigned to the alkyne proton.

Deprotection of acetylated group sodium methoxide and purification by Sephadex LH-20 size exclusion chromatographies provided pure **CnGlu3** facial amphiphiles as white powder which

Table 1 Physico-chemical properties of tripods

Entry	CAC ^a /mM	$\gamma_{\text{CAC}}^a/\text{mN m}^{-1}$	$A_{\text{min}}/\text{\AA}^2$ ^a	P^c	$\log K'_{\text{W}}^b$	D_{h}/nm^c	%Vol	N_{Agg}^d	R_{g}/nm^d
C3Glu3	2.38 ± 0.03	39.2 ± 0.2	235 ± 58	0.260	6	3.3	99.9	3	1.4
C4Glu3	0.84 ± 0.05	36.3 ± 0.2	211 ± 26	0.292	5.9	5.2	99.8	5	1.8
C5Glu3	0.13 ± 0.01	35.8 ± 0.2	210 ± 8	0.295	7.4	8.1	99.9	13	3.6
C6Glu3	0.01 ± 0.001	33.2 ± 0.2	192 ± 24	0.324	8.5	11.5	99.8	n.d.	n.d.
C7Glu3	$1.2 \times 10^{-3} \pm 0.1 \times 10^{-3}$	31.3 ± 0.2	211 ± 13	0.296	9.6	>200	52	n.d.	n.d.

^a Measured by tensiometry (Wilhelmy plate method). Each value is the mean of three different measurements ± SD. ^b Measured by reversed phase HPLC. ^c The hydrodynamic or Stokes diameter (D_{h}) of particles is measured at a concentration at least 15 times above the CAC. The values are the average of 10 runs. ^d Aggregation number (N_{Agg}) and radius of gyration (R_{g}) measured by SAXS at a concentration about 15 times the CAC ^e Packing parameter.

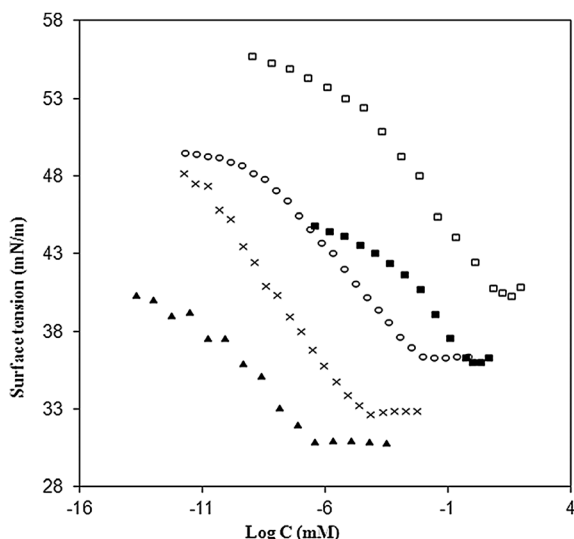


Fig. 2 Surface tension vs. $\log C$ for compounds **C3Glu3** (□), **C4Glu3** (■), **C5Glu3** (○), **C6Glu3** (×) and **C7Glu3** (▲).

were fully characterized by ¹H, ¹³C and HR mass spectrometry. All these compounds have good water solubility except **C7Glu3**; this lower solubility was associated with the longer hydrocarbon tails of the lipophilic part.

Tensiometric measurements allowed us to determine the main tensioactive properties of these tripods (Table 1 and Fig. 2). For all compounds tested, the surface tension is observed

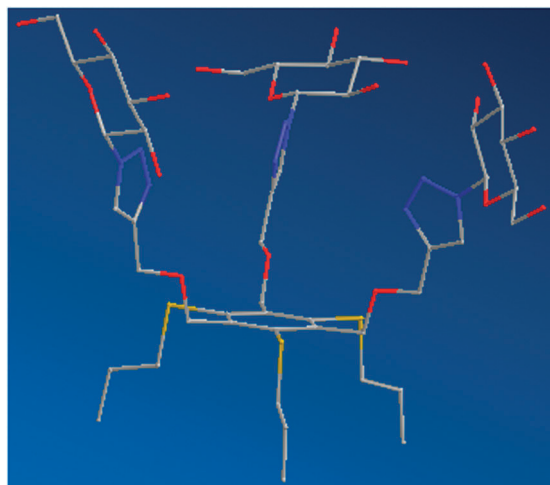
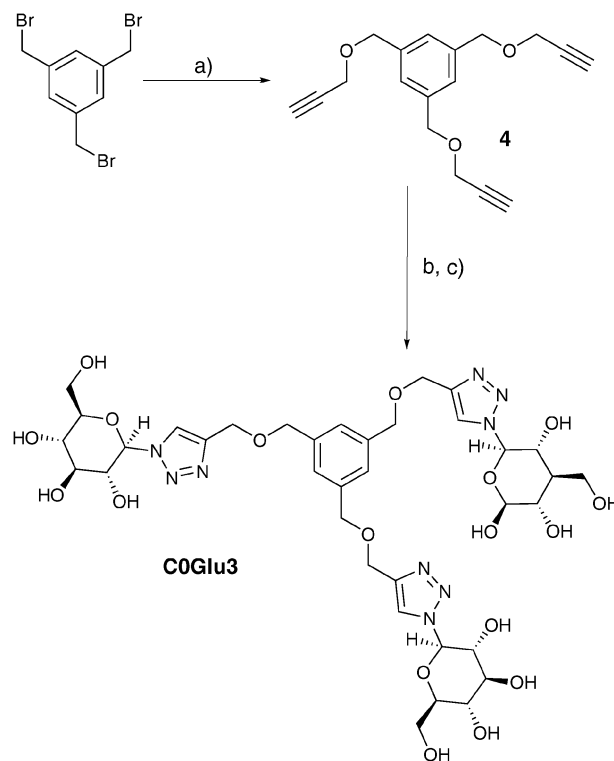


Fig. 3 Representation of a stick molecular model of the tripod **C3Glu3** (Chem3D Pro 11.0).

to linearly decrease as tripod concentration increases, showing breaks corresponding to the critical aggregation concentration (CAC) depending on the hydrophobic chain length, as for a conventional surfactant.²⁴

Such behavior clearly indicates a facial segregation of polar and apolar parts in water on both sides of the aromatic ring (Fig. 3). Furthermore, it should be noted that the triglucosylated compound without hydrocarbon chains (**C0Glu3**) prepared from 1,3,5-tris(bromomethyl)benzene following synthetic routes, summarized in Scheme 2, does not exhibit surfactant properties, indicating that the aromatic ring alone was not enough to endow the molecule with a sufficiently hydrophobic character.

For the tripod compounds (Fig. 4), $\log(\text{CAC})$ linearly decreases when the number of methylenes of each hydrophobic chain increases: $\log(\text{CAC}) = -1.96nC + 7.26$ with $R^2 = 0.9804$. However it should be pointed out that within a homologous



Scheme 2 Synthetic route of **C0Glu3**, reagents, temperature, time and yield: (a) propargyl alcohol, NaH 60%, DMF, 0 °C, 48%; (b) 1-azido-1-deoxy- β -D-glucopyranoside tetraacetate, DIEA, CuI, THF, RT, 50%; (c) MeONa cat., MeOH/THF (4:1), pH 9–10, rt., 24 h, 87%.

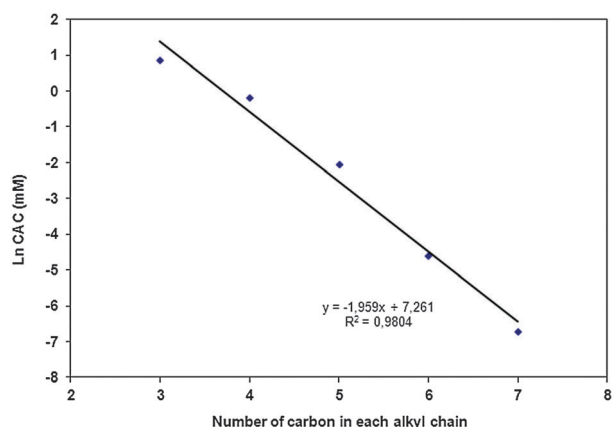


Fig. 4 logCAC plotted vs. number of carbons of the hydrophobic chains.

series of surfactants, the CAC usually decreases by a factor of about 10 every time two methylene groups are added to the hydrophobic tail.²⁴ In the present case, this factor increases from three to eight every time one methylene group is added to each tail. This weaker contribution to the hydrophobic effect is explained by the fact that the three methylenes are not added linearly to one chain, but to three different chains. Similar behavior can be observed with lipids. A second hydrocarbon chain added to an amphiphilic molecule makes a smaller contribution to the hydrophobic effect than the one already linked to that molecule.²⁴ By applying Gibbs equation $\Gamma = -(1/RT)[d\gamma/d\text{Log } C]$, the relative excess of surfactant at the air–water interface Γ was determined, leading to the evaluation of the area per surfactant polar head from $A_{\text{min}} = 1/\Gamma N$. These tripod surfactants exhibit a wide polar head ($A_{\text{min}} = 210 \pm 60 \text{ \AA}^2$), whatever the nature of the hydrophobic tails (Table 1).

$\log(K'w)$ is a parameter closely related to the molecule's water/octanol partition coefficient, which can be obtained from reverse-phase HPLC.²⁵ This parameter is usually considered to reflect the hydrophobic character of the surfactant. $\log(K'w)$ shows a linear evolution from **C4Glu3** to **C7Glu3** when the carbon number of hydrophobic chains increases (Fig. 5). It can be seen that the $\log(K'w)$ of the **C3Glu3** compound is equal to that of the **C4Glu3** compound. Thus, we can assume that the hydrophobic contribution of the 3 additional methylenes remained marginal for very short chains. Above their CAC, all surfactants form monodispersed self-assembled systems with a Stokes (or hydrodynamic) diameter lower than 20 nm, except for **C7Glu3** (Table 1 and Fig. 6). The tripod hydrodynamic diameters increase with the length of the hydrophobic tail. Particle diameters obtained from DLS measurements suggest that **C3Glu3** and **C4Glu3** should form spherical micelles in water with a diameter of less than 6 nm, but the increase in the particle size observed with **C5Glu3** and **C6Glu3** indicates the formation of larger micelles.

Further information about the shape of the tripod assemblies was obtained by Small Angle X-ray Scattering experiments (SAXS). The last tripod **C7Glu3**, which has low water solubility, leads to unstable large particles larger than 0.2 μm as observed by TEM after negative staining (see ESI†, Fig. S1). Moreover, this compound precipitates quickly after dispersion by sonication. DLS measurements also reveal very large aggregates testifying to the rapid fusion of vesicles formed from the tripod **C7Glu3**.

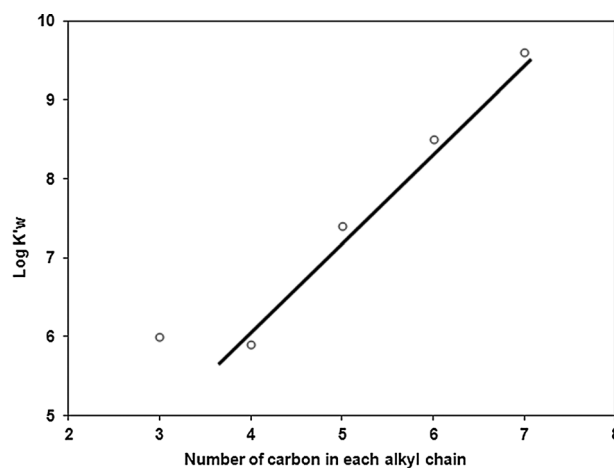


Fig. 5 Log($K'w$) of tripods **CnGlu3** plotted against number of carbon of the hydrophobic chains.

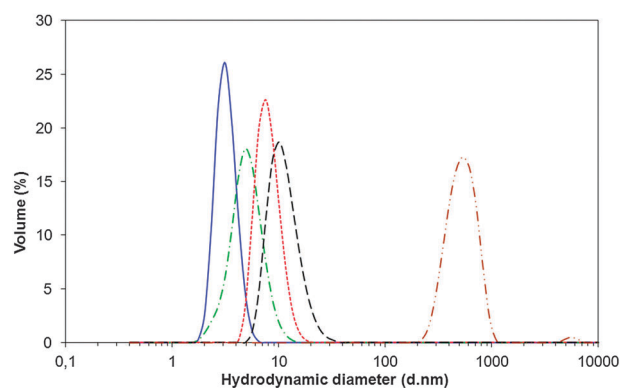


Fig. 6 Stokes (or hydrodynamic) diameter distribution from DLS measurements for amphiphile solutions as a function of length of linear alkyl chains: **C3Glu3** at 15 CMC (—, blue), **C4Glu3** at 15 CMC (—, green), **C5Glu3** at 120 CMC (···, red), **C6Glu3** at 15 CMC (---, black), **C7Glu3** at 120 CMC (— · —, brown).

To better understand the whole process of evolution, the self-aggregated properties of **C3-** to **C5Glu3** tripods having good water solubility were studied by SAXS at different concentrations. Different behaviours were observed for **C3-** to **C5Glu3** tripods as the hydrophobic tail increased in length. Comparisons between **C3**, **C4** and **C5Glu3** at the same concentration (about 40 g L^{-1}) are shown in Fig. 7A. Evolution of scattering from factors of **C3Glu3** to **C5Glu3** as a function of concentration is shown in the ESI† (Fig. S2). As the concentration increases up to 42 g L^{-1} (15CMC), **C3Glu3** and **C4Glu3** form small aggregates (see ESI†, Table S2), probably trimers for **C3Glu3** and larger aggregates for **C4Glu3**. Radii of gyration and molecular masses have been determined *via* the Guinier approximation, the latter being determined by comparing the forward scattering intensity value $I(0)$ at the highest concentration with the $I(0)$ value below the CAC (taken to be monomeric). Analysis of the pair distribution function $P(r)$ for **C3Glu3** using the program GNOM²⁶ yielded a maximum particle dimension D_{max} of about 4 nm, consistent with DLS measurements. In the case of **C4Glu3**, although the evolution is essentially the same, it

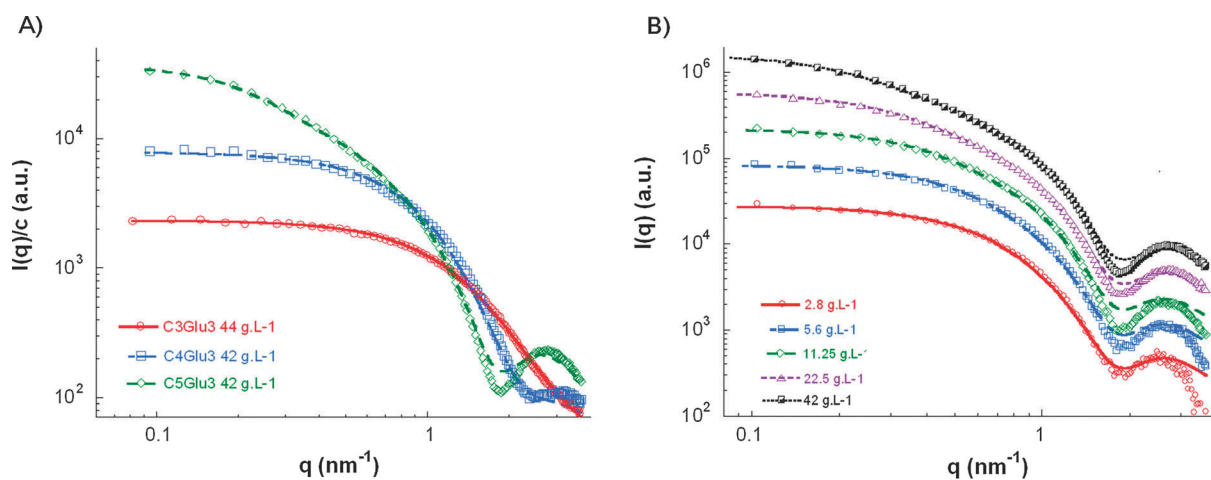


Fig. 7 (A) Experimental SAXS curves of **C3-** to **C5Glu3** at their highest concentrations. (B) Scattering intensities of **C5Glu3** at different concentrations. The curves are not normalized for sake of clarity. The symbols represent the experimental data and the lines the data fits.

was impossible to characterize the monomeric form below the CAC due to a poor SAXS signal below 0.9 g L^{-1} .

In the case of **C5Glu3**, the scattering curves clearly present a different behaviour. The **C5Glu3** pair distribution functions (see ESI†, Fig. S3) and the Guinier analysis suggest the formation of elongated objects, which lengthen as the tripod concentration increases. The increase in intensity at very low angles confirms the presence of larger objects, as compared to **C3Glu3** and **C4Glu3**. The SAXS curves were fitted using least-square models, for **C3-** to **C5Glu3** at the same high concentration (Fig. 7A) and for **C5Glu3** as a function of concentration (Fig. 7B). By using a model of a generalized Gaussian coil, **C3Glu3** looks like an oblate ellipsoid. For **C4Glu3** and **C5Glu3**, a model of rod-like copolymer micelles has been used, which shows that **C4Glu3** is thinner and shorter than **C5Glu3** at their highest concentration, but thicker than **C3Glu3**. Cross-sectional radius ($1.52 \pm 0.04 \text{ nm}$), radius of gyration and length were therefore determined for each **C5Glu3** concentration (see ESI†, Table S2). SAXS measurements (R_g and D_{max}) are in accordance with dynamic light scattering measurements in terms of evolution of particle dimensions as the hydrophobic tail increases in length. In the case of **C3-** and **C4Glu3**, DLS is not able to distinguish between the different species in solution (monomer and small aggregates), and gives only an average hydrodynamic diameter of tripods in solution. For **C5Glu3**, the DLS diameter is slightly lower than the length determined by SAXS, since for very long cylinders the diffusion and therefore the hydrodynamic radius are mainly determined by the diameter of the rod, and not by its length.²⁷ Differences in behaviour among **C3Glu3**, **C4Glu3** and **C5Glu3** have yet to be clearly explained. SAXS studies on **C6Glu3** and **C7Glu3** would probably have shed further light on tripod self-assembly, but their solubility was too low for SAXS experiments.

An interesting question is whether the results obtained by SAXS studies confirm the concept of the *molecular packing parameter* introduced by Tanford.²⁸

According to this theory, a simple and common conceptual way of relating the geometric shape of an amphiphile and the

preferred type of aggregation is through the surfactant packing parameter.

$$P = v/al \quad (1)$$

where v is the volume of the chain, l is the length of the chain and a , the cross-sectional area of the head group. Cross-sectional head group areas were determined from CMC measurements as described in the Experimental section. For single-chain hydrocarbon tails, both the length of the chain and its volume can be estimated according to Tanford:

$$v = 3(27.4 + 26.9n) \quad (2)$$

$$l = 1.5 + 1.265n \quad (3)$$

where l is the length of the fully extended chain in Å, v the volume of the 3 alkyl chains in Å³, and n the number of hydrocarbon units in each chain.

Tanford *et al.* studied the factors determining the packing patterns of amphiphilic molecules and the shape of aggregates. Amphiphiles having $P < 1/3$ prefer to form spherical micelles while those having either $1/3 < P < 1/2$ or $1/2 < P < 1$, prefer to form either rod-like or cylindrical micelles, or lamellar phases, respectively. We can observe for all compounds (Table 1) that the calculated values for each compound show small changes in the critical packing parameter. The general trend predicted by the molecular packing parameter does not seem valid for our new tripod facial surfactants. Actually, this predictive theory is valid if the micelle core is packed with surfactant tails leaving no empty space.²⁹ The volume occupied by the hydrophobic part is certainly greater than that calculated with eqn (2) because there is an empty space between the 3 chains due to the presence of the rigid aromatic central core of this new family of tensioactives. Trappman *et al.* pointed out that the interaction of space-demanding dendritic amphiphiles dominates their self-assembly process.³⁰ Kratzat and Finkelmann have also reported that asymmetrically branched non-ionic surfactants do not follow the packing parameter model of Tanford.³¹ Due to the very low aggregation number of compounds **C3Glu3**, **C4Glu3** and **C5Glu3** measured by SAXS, the aggregation properties of

these compounds appear to be similar to those of bile salts.³² In contrast to classical detergents, where the hydrophilic head group and the lipophilic flexible aliphatic chains are clearly separated, bile salt molecules have a lipophilic surface, which is the convex side of the rigid steroid ring system and a hydrophilic surface which is the polyhydroxylated concave side of the molecule. Bile salt micelles also have much smaller aggregation numbers than classical detergent micelles. Moreover, it is interesting to note that bile salts behave quite differently in water from classical detergents.³³ They form two types of aggregates, small aggregates and much larger ones. Small aggregates with an aggregation number of less than 10 lead to the formation of primary micelles of almost spherical shapes which transform with increasing tensioactive concentration into secondary micelles with rod-like structures. The results obtained by SAXS measurement with **C5Glu3** suggest an association behaviour of this amphiphilic tripods equivalent to that of bile salts with a face-to-face arrangement of the hydrophobic parts and the formation of rod-shaped micelles whose length increases as a function of the surfactant concentration (see ESI† in Table S2).

Conclusion

The synthetic route chosen for the synthesis of these new benzene-based facial amphiphiles allows the selective introduction in good yield of hydrophilic and hydrophobic parts of the molecule. Thus, both overall electrical charges and/or water solubility of the polar head and nature and length of hydrophobic parts can be tuned easily. We show that the increased number of small lipophilic chains and their segregation on one side of these amphiphilic compound tripods afford them tensioactive properties. Whatever the length of the hydrocarbon part, these amphiphilic compounds exhibit self-aggregation properties in water. They lead to particles whose size and shape are closely dependent on the length of the hydrophobic tail. Long hydrocarbon chains (**C7Glu3**) decrease tripod solubility in water, and thus their ability to form small aggregates. The attachment of other types of hydrophilic groups on the polar face of these tripods should easily offset hydrophobicity, modulate the hydrophilic lipophilic balance and solve problems of water solubility. We use SAXS experiments to characterize two different behaviours in the self-aggregation of **CnGlu3** tripods. The tripods form aggregates whose size and shape depend on the length of the hydrophobic tail. Interestingly, although the aggregation numbers, N_{agg} , of these facial amphiphiles are very low, this aggregation behaviour in water is close to that of natural facial surfactants such as bile salt derivatives. The aggregation process of **C5Glu3** seems to proceed stepwise over a broad concentration range, as with bile salt detergents. The design of these tripod facial surfactants and their ability to interact face-to-face with the hydrophobic part suggest that they are suitable for use in the solubilization of large hydrophobic nanoparticles. The study of their ability to handle and pinch-off specifically hydrophobic nanoparticles in aqueous solution is currently in progress.

General method

All starting materials were commercially available and were used without further purification. All solvents were of reagent

grade and used as received unless stated. THF and MeOH were dried over Na and CH_2Cl_2 over CaH_2 under argon atmosphere. Commercially anhydrous DMF was stored over activated molecular sieves of 3 Å. The progress of the reactions was monitored by thin layer chromatography (TLC, Merck 254, silica plates) and the compounds were detected either by exposure to ultraviolet light (254 nm) or by spraying with a 0.05% permanganate aqueous solution or with an acidic solution of ceric molybdate following heating at 150 °C. Flash chromatography purifications were carried out on silica gel (40–63 µm granulometry). Size exclusion chromatography purifications were carried out on a Sephadex LH-20 resin. ^1H and ^{13}C spectra were recorded on a Bruker AC 250 spectrometer at 250 MHz for ^1H and 62.86 MHz for ^{13}C . Chemical shifts (δ values) were reported in ppm downfield from internal residual solvent as a heteronuclear reference. HRMS(ESI) was determined on a QStar Elite mass spectrometer.

Synthesis

1,3,5-Tris(chloromethyl)-2,4,6-tris(propylthio)benzene (2a). To a solution of potassium *tert*-butoxide (2.27 g, 20.23 mmol) in DMI (30 mL) was added under argon atmosphere propanethiol (3.8 mL, 21.76 mmol). The solution was stirred for 10 min then compound **1** (2.28 g, 5.63 mmol) was added and the thick mixture was stirred for 16 h at room temperature. The reaction mixture was poured into water (300 mL) and extracted with AcOEt (3 × 100 mL). The organic layer was washed first with H_2O (2 × 50 mL), then with brine (50 mL), dried with anhydrous MgSO_4 , filtered and concentrated. The crude compound was subjected to flash chromatography on a silica gel column with AcOEt/cyclohexane (2 : 8), giving the tris(hydroxymethyl) benzenic product as colorless oil (1.43 g, 97%). R_f 0.24 in AcOEt/cyclohexane (3 : 7). ^1H NMR (CDCl_3) δ 1.03 (t, $^3J = 7.34$ Hz, 9H), 1.65 (six, $^3J = 7.39$ Hz, 6H), 2.89 (t, $^3J = 7.55$ Hz, 6H), 2.9 (br s, 3H), 5.31 (s, 6H). ^{13}C NMR (CDCl_3) δ 13.5, 23.0, 40.7, 63.3, 137.2, 150.7.

Et_3N (1.25 mL, 9 mmol) was added slowly to a solution of the tris(hydroxymethyl)benzene derivative (1.2 g, 2 mmol) in dry CH_2Cl_2 (30 mL) cooled with an ice bath at 5 °C under argon atmosphere. Methane sulfonyl chloride (610 µL, 7.8 mM) was added dropwise at 5 °C and the reaction mixture was stirred for 48 h at room temperature. The reaction mixture was monitored by TLC with CH_2Cl_2 /cyclohexane (1 : 9) as eluent until only one spot was obtained, and then concentrated to give a crude compound as an orange oil. Purification by flash chromatography on a silica gel column with CH_2Cl_2 /cyclohexane (1 : 9) gave the expected product as a white powder (1.09 g, 83%), R_f 0.53 in CH_2Cl_2 /cyclohexane (1 : 9), Mp 88.7–89.1 °C. ^1H NMR (CDCl_3) δ 1.07 (t, $^3J = 7.36$ Hz, 9H), 1.72 (six, $^3J = 7.36$ Hz, 6H), 3.02 (t, $^3J = 7.36$ Hz, 6H), 5.51 (s, 6H). ^{13}C NMR (CDCl_3) δ 13.6, 23.1, 40.9, 46.2, 139.9, 149.5. HRMS (ESI⁺) calcd for $\text{C}_{18}\text{H}_{28}\text{Cl}_3\text{S}_3$ ($[\text{M} + \text{H}]^+$) 445.0436, found 445.0419.

Compounds **2b–2e** were obtained as described previously for **2a** from 5.63 mmol of compound **1** by using the appropriate thiol (butane-, pentane-, hexane- or heptanethiol) instead of propane thiol.

1,3,5-Tris(chloromethyl)-2,4,6-tris(butylthio)benzene (2b). Yield 865 mg (88%), colorless oil, R_f 0.5 in CH_2Cl_2 /cyclohexane (1 : 9).

^1H NMR (CDCl_3) δ 0.96 (t, $^3J = 7.32$ Hz, 9H), 1.49 (six, $^3J = 7.3$ Hz, 6H), 1.69 (six, $^3J = 6.73$ Hz, 6H), 3.04 (t, $^3J = 7.53$ Hz, 6H), 5.51 (s, 6H). ^{13}C NMR (CDCl_3) δ 13.7, 22.1, 31.6, 38.7, 46.2, 140.0, 149.5. HRMS (ESI^+) calcd for $\text{C}_{21}\text{H}_{34}\text{Cl}_3\text{S}_3$ ($[\text{M} + \text{H}]^+$) 487.0936, found 487.0888.

1,3,5-Tris(chloromethyl)-2,4,6-tris(pentylthio)benzene (2c). Yield 925 mg (87%), colorless oil, R_f 0.56 in $\text{CH}_2\text{Cl}_2/\text{cyclohexane}$ (1:9). ^1H NMR (CDCl_3) δ 0.93 (t, $^3J = 7.12$ Hz, 9H), 1.32–1.46 (m, 12H), 1.71 (p, $^3J = 7.49$ Hz, 6H), 3.03 (t, $^3J = 7.63$ Hz, 6H), 5.51 (s, 6H). ^{13}C NMR (CDCl_3) δ 14.0, 22.3, 29.3, 31.1, 39.0, 46.2, 140.0, 149.5. HRMS (ESI^+) calcd for $\text{C}_{24}\text{H}_{40}\text{Cl}_3\text{S}_3$ ($[\text{M} + \text{H}]^+$) 529.1328, found 529.1358.

1,3,5-Tris(chloromethyl)-2,4,6-tris(hexylthio)benzene (2d). Yield 1.03 g (91%), colorless oil, R_f 0.66 in $\text{CH}_2\text{Cl}_2/\text{cyclohexane}$ (1:9). ^1H NMR (CDCl_3) δ 0.91 (t, $^3J = 6.73$ Hz, 9H), 1.29–1.47 (m, 18H), 1.7 (p, $^3J = 7.8$ Hz, 6H), 3.02 (t, $^3J = 7.4$ Hz, 6H), 5.51 (s, 6H). ^{13}C NMR (CDCl_3) δ 14.1, 22.5, 28.6, 29.5, 31.4, 39.0, 46.2, 140.0, 149.5. HRMS (ESI^+) calcd for $\text{C}_{27}\text{H}_{46}\text{Cl}_3\text{S}_3$ ($[\text{M} + \text{H}]^+$) 571.1854, found 571.1827.

1,3,5-Tris(chloromethyl)-2,4,6-tris(heptylthio)benzene (2e). Yield 993 mg (81%), colorless oil, R_f 0.38 in $\text{CH}_2\text{Cl}_2/\text{cyclohexane}$ (1:9). ^1H NMR (CDCl_3) δ 0.91 (t, $^3J = 6.73$ Hz, 9H), 1.31–1.44 (m, 24H), 1.71 (p, $^3J = 7.65$ Hz, 6H), 3.03 (t, $^3J = 7.63$ Hz, 6H), 5.51 (s, 6H). ^{13}C NMR (CDCl_3) δ 14.1, 22.7, 28.6, 28.9, 29.0, 29.3, 29.6, 31.8, 39.0, 46.2, 140.0, 149.5. HRMS (ESI^+) calcd for $\text{C}_{30}\text{H}_{52}\text{Cl}_3\text{S}_3$ ($[\text{M} + \text{H}]^+$) 613.2203, found 613.2234.

1,3,5-Tris(prop-2-ynyloxymethyl)-2,4,6-tris(propylthio)benzene (3a). To a solution of propargyl alcohol (210 μL , 3.6 mmol) in anhydrous DMF (5 mL) cooled to 0 $^\circ\text{C}$ was slowly added NaH (60% w/w, oil dispersion) (144 mg, 3.6 mM) under argon. The reaction mixture was stirred for 10 min and a solution of **2a** (656 mg, 1 mmol) in dry THF (5 mL) was slowly added at 0 $^\circ\text{C}$. The resulting mixture was stirred for 18 h at room temperature. Then ice was added. The mixture was poured into water (50 mL) and extracted with AcOEt (3 \times 50 mL). The organic layers were gathered, washed first with H_2O (2 \times 30 mL), then with brine (30 mL), dried with anhydrous MgSO_4 , filtered and concentrated. Purification by flash chromatography on a silica gel column with $\text{CH}_2\text{Cl}_2/\text{cyclohexane}$ (6:4) as eluent gave the expected product as yellow oil (329 mg, 65%). R_f 0.36 in $\text{CH}_2\text{Cl}_2/\text{cyclohexane}$ (8:2). ^1H NMR (CDCl_3) δ 1.02 (t, $^3J = 7.34$ Hz, 9H), 1.6 (p, $^3J = 7.34$ Hz, 6H), 2.5 (t, $^4J = 2.38$ Hz, 3H), 2.88 (t, $^3J = 7.24$ Hz, 6H), 4.34 (d, $^4J = 2.35$ Hz, 3H), 5.33 (s, 6H). ^{13}C NMR (CDCl_3) δ 13.6, 23.0, 41.0, 58.1, 71.6, 74.4, 79.9, 141.4, 147.0.

Compounds **3b–3e** were obtained as described previously for **3a** by using the appropriate 1,3,5-tris(chloromethyl)-2,4,6-tris(alkylthio)benzene **2b–2e** (0.5 mmol) instead of **2a**.

1,3,5-Tris(prop-2-ynyloxymethyl)-2,4,6-tris(butylthio)benzene (3b). Yield 339 mg (62%), yellow oil, R_f 0.43 in $\text{CH}_2\text{Cl}_2/\text{cyclohexane}$ (7:3). ^1H NMR (CDCl_3) δ 0.92 (t, $^3J = 7.2$ Hz, 9H), 1.44 (six, $^3J = 8.0$ Hz, 6H), 1.57 (p, $^3J = 7.01$ Hz, 3H), 2.49 (t, $^4J = 2.37$ Hz, 3H), 2.9 (t, $^3J = 7.5$ Hz, 6H), 4.33 (d, $^4J = 2.39$ Hz, 6H), 5.3 (s, 6H). ^{13}C NMR (CDCl_3) δ 14.1, 22.6, 29.6, 39.1, 58.1, 71.6, 74.4, 79.9, 141.4, 147.0.

1,3,5-Tris(prop-2-ynyloxymethyl)-2,4,6-tris(pentylthio)benzene (3c). Yield 492 mg (84%), yellow oil, R_f 0.45 in $\text{CH}_2\text{Cl}_2/\text{cyclohexane}$ (6:4). ^1H NMR (CDCl_3) δ 0.9 (t, $^3J = 7.06$ Hz, 9H), 1.29–1.42 (m, 12H), 1.58 (m, 6H), 2.49 (t, $^4J = 2.32$ Hz, 3H), 2.89 (t, $^3J = 7.49$ Hz, 6H), 4.33 (d, $^4J = 2.36$ Hz, 6H), 5.3 (s, 6H). ^{13}C NMR (CDCl_3) δ 14.0, 22.3, 29.4, 31.2, 39.0, 58.1, 71.6, 74.4, 79.9, 141.4, 147.0.

1,3,5-Tris(prop-2-ynyloxymethyl)-2,4,6-tris(hexylthio)benzene (3d). Yield 488 mg (77%), yellow oil, R_f 0.45 in $\text{CH}_2\text{Cl}_2/\text{cyclohexane}$ (6:4). ^1H NMR (CDCl_3) δ 0.9 (t, $^3J = 6.81$ Hz, 9H), 1.26–1.43 (m, 18H), 1.59 (p, $^3J = 8.88$ Hz, 6H), 2.49 (t, $^4J = 2.37$ Hz, 3H), 2.89 (t, $^3J = 7.5$ Hz, 6H), 4.33 (d, $^4J = 2.39$ Hz, 6H), 5.3 (s, 6H). ^{13}C NMR (CDCl_3) δ 14.1, 22.6, 28.7, 29.6, 31.5, 39.1, 58.1, 71.6, 74.4, 79.9, 141.4, 147.0.

1,3,5-Tris(prop-2-ynyloxymethyl)-2,4,6-tris(heptylthio)benzene (3e). Yield 452 mg (67%), yellow oil, R_f 0.45 in $\text{CH}_2\text{Cl}_2/\text{cyclohexane}$ (6:4). ^1H NMR (CDCl_3) δ 0.9 (t, $^3J = 6.88$ Hz, 9H), 1.27–1.4 (m, 24H), 1.59 (p, $^3J = 8.88$ Hz, 6H), 2.49 (t, $^4J = 2.37$ Hz, 3H), 2.89 (t, $^3J = 7.5$ Hz, 6H), 4.33 (d, $^4J = 2.39$ Hz, 6H), 5.3 (s, 6H). ^{13}C NMR (CDCl_3) δ 14.1, 22.6, 28.7, 29.6, 31.5, 39.1, 58.1, 71.6, 74.4, 79.9, 141.4, 147.0.

1,3,5-Tris[1-(β -D-glucopyranosyl)-1,2,3-triazole-4-yloxymethyl]-2,4,6-tris(propylthio)benzene (C3Glu3). To a solution of **3a** (358 mg, 0.5 mmol) in THF (15 mL) at room temperature was added 2,3,4,6-tetra-*O*-acetyl- β -D-glucopyranosyl azide (740 mg, 1.8 mmol), DIEA (520 μL , 3 mmol) and CuI (29 mg, 0.15 mmol). The resulting green mixture was stirred for 24 h at room temperature. AcOEt (60 mL) was then added and the organic layer was washed first with saturated aqueous NH_4Cl (3 \times 20 mL), then with brine (20 mL), dried with anhydrous MgSO_4 , filtered and concentrated. The crude solid was subjected to flash chromatography on a silica gel column with a gradient of AcOEt/ CH_2Cl_2 (1:9 to 4:6), giving the acetylated product as a white powder (677 mg, 83%). R_f 0.26 in AcOEt/ CH_2Cl_2 (4:6). Mp 190.1–192.9 $^\circ\text{C}$. $[\alpha]_{\text{D}}^{25} = -56.2$ (*c* 1, CH_2Cl_2). ^1H NMR (CDCl_3) δ 0.92 (t, $^3J = 7.41$ Hz, 9H), 1.53 (six, $^3J = 7.4$ Hz, 6H), 1.88 (s, 9H), 2.05–2.09 (3s, 27H), 2.79 (t, $^3J = 7.41$ Hz, 6H), 4.02 (ddd, $^3J = 2.82$ Hz, $^3J = 4.76$ Hz, $^3J = 9.98$ Hz, 3H), 4.14 (dd, $^3J = 2$ Hz, $^2J = 12.53$ Hz, 3H), 4.3 (dd, $^3J = 4.95$ Hz, $^2J = 12.56$ Hz, 3H), 4.82 (s, 6H), 5.21–5.33 (m, 9H), 5.4–5.53 (m, 6H), 5.9 (d, $^3J = 9.0$ Hz, 3H), 7.83 (s, 3H). ^{13}C NMR (CDCl_3) δ 14.0, 20.2, 20.6, 20.7, 23.0, 40.8, 61.6, 64.2, 67.7, 70.2, 72.0, 72.8, 75.0, 85.7, 121.1, 141.1, 146.0, 147.1, 168.9, 169.4, 170.0, 170.6.

Deacetylated compound. An acetylated compound (550 mg, 0.3 mmol) was dissolved in 50 mL of a dry mixture of THF/MeOH (1:4). A sufficient catalytic quantity of sodium methoxide was added to reach a pH of 9–10 and the reaction mixture was stirred for 24 h at room temperature. The solution was neutralized with the resin acid IRC-50 (pH = 7), filtered and concentrated. The solid was purified by Sephadex LH-20 size exclusion chromatography with methanol, giving the expected product as a white powder (246 mg, 73%). R_f 0.18 in AcOEt/MeOH/ H_2O (7:2:1). Mp 182.8–184.1 $^\circ\text{C}$. $[\alpha]_{\text{D}}^{25} = -8.0$ (*c* 1, MeOH). HRMS (ESI^+) calcd for $\text{C}_{45}\text{H}_{71}\text{N}_9\text{O}_{18}\text{S}_3$ ($[\text{M} + 2\text{H}]^{2+}$): 560.7034, found 560.7033. ^1H NMR (DMSO) δ 0.90 (t, $^3J = 7.4$ Hz, 9H), 1.45 (six, $^3J = 7.23$ Hz, 6H),

2.79 (t, $^3J = 7.28$ Hz, 6H), 3.23 (m, 3H), 3.37–3.48 (m, 9H), 3.66–3.77 (m, 6H), 4.63 (t, $^3J = 7.5$ Hz, 3H), 4.69 (s, 6H), 5.18 (d, $^3J = 5.36$ Hz, 3H), 5.19 (s, 6H), 5.3 (d, $^3J = 4.81$ Hz, 3H), 5.37 (d, $^3J = 6.06$ Hz, 3H), 5.53 (d, $^3J = 9.23$ Hz, 3H), 8.27 (s, 3H). ^{13}C NMR (DMSO) δ 13.8, 22.9, 39.0, 61.6, 64.2, 70.0, 71.8, 72.5, 77.4, 80.4, 87.9, 123.6, 140.4, 144.1, 147.3.

Compounds **CnGlu3** were obtained as previously described for the synthesis of **C3Glu3** by using the appropriate 1,3,5-tris(prop-2-ynyloxymethyl)-2,4,6-tris(alkylthio)benzene **3b–3e** (0.5 mmol) instead of **3a**, then 0.3 mmol of acetylated compound.

1,3,5-Tris[1-(β -D-glucopyranosyl)-1,2,3-triazole-4-yloxymethyl]-2,4,6-tris(butylthio) benzene (**C4Glu3**)

Acetylated compound. Yield 627 mg (75%), white powder, R_f 0.32 in AcOEt/CH₂Cl₂ (4:6). Mp 194.3–195.9 °C. $[\alpha]_D^{25} = -54.9$ (*c* 1, CH₂Cl₂). ^1H NMR (CDCl₃) δ 0.86 (t, $^3J = 7.12$ Hz, 6H), 1.34 (six, $^3J = 7.65$ Hz, 6H), 1.45–1.68 (m, 6H), 1.9 (s, 9H), 2.04–2.09 (3s, 27H), 2.81 (t, $^3J = 7.41$ Hz, 6H), 4.02 (m, 3H), 4.14 (dd, $^3J = 1.73$ Hz, $^2J = 12.55$ Hz, 3H), 4.3 (dd, $^3J = 4.85$ Hz, $^2J = 12.62$ Hz, 3H), 4.83 (s, 6H), 5.22–5.33 (m, 9H), 5.4–5.53 (m, 6H), 5.9 (d, $^3J = 8.75$ Hz, 3H), 7.84 (s, 3H). ^{13}C NMR (CDCl₃) δ 13.7, 20.2, 20.6, 20.7, 22.1, 31.7, 38.6, 61.6, 64.2, 67.7, 70.3, 72.0, 72.8, 75.0, 85.7, 121.1, 141.1, 146.0, 147.1, 168.8, 169.4, 170.0, 170.5.

Deacetylated compound. Yield 289 mg (87%), white powder, R_f 0.4 in AcOEt/MeOH/H₂O (7:2:1). Mp 184.3–186.0 °C. $[\alpha]_D^{25} = -8.4$ (*c* 1, MeOH). HRMS (ESI⁺) calcd for C₄₈H₇₇N₉O₁₈S₃ ([M + 2H]²⁺): 581.7269, found 581.7275. ^1H NMR (DMSO) δ 0.82 (t, $^3J = 7.03$ Hz, 9H), 1.26–1.41 (m, 12H), 2.81 (t, $^3J = 6.91$ Hz, 6H), 3.22 (m, 3H), 3.37–3.46 (m, 9H), 3.67–3.79 (m, 6H), 4.63 (t, $^3J = 5.09$ Hz, 3H), 4.69 (s, 6H), 5.19 (s, 9H), 5.31 (d, $^3J = 4.49$ Hz, 3H), 5.36 (d, $^3J = 5.96$ Hz, 3H), 5.53 (d, $^3J = 9.2$ Hz, 3H), 8.25 (s, 3H). ^{13}C NMR (DMSO) δ 14.1, 21.9, 31.7, 38.0, 61.2, 64.2, 70.0, 71.8, 72.6, 77.4, 80.4, 87.9, 123.5, 140.4, 144.1, 147.3.

1,3,5-Tris[1-(β -D-glucopyranosyl)-1,2,3-triazole-4-yloxymethyl]-2,4,6-tris(pentylthio) benzene (**C5Glu3**)

Acetylated compound. Yield 685 mg (79%), white powder, R_f 0.42 in AcOEt/CH₂Cl₂ (4:6). Mp 179.5–181.2 °C. $[\alpha]_D^{25} = -55.9$ (*c* 1, CH₂Cl₂). ^1H NMR (CDCl₃) δ 0.86 (t, $^3J = 7.1$ Hz, 9H), 1.25–1.31 (m, 12H), 1.5 (p, $^3J = 7.26$ Hz, 6H), 1.88 (s, 9H), 2.05–2.08 (3s, 27H), 2.8 (t, $^3J = 7.41$ Hz, 6H), 4.02 (m, 3H), 4.14 (dd, $^3J = 1.98$ Hz, $^2J = 12.55$ Hz, 3H), 4.3 (dd, $^3J = 4.83$ Hz, $^2J = 12.52$ Hz, 3H), 4.81 (s, 6H), 5.21–5.32 (m, 9H), 5.39–5.52 (m, 6H), 5.9 (d, $^3J = 8.93$ Hz, 3H), 7.83 (s, 3H). ^{13}C NMR (CDCl₃) δ 14.0, 20.2, 20.6, 20.7, 22.3, 29.3, 31.1, 38.9, 61.6, 64.2, 67.7, 70.0, 71.9, 72.7, 75.0, 85.7, 121.1, 141.1, 146.0, 147.1, 168.8, 169.4, 170.0, 170.6.

Deacetylated compound. Yield 346 mg (95%), white powder, R_f 0.46 in AcOEt/MeOH/H₂O (7:2:1). Mp 187.8–189.3 °C. $[\alpha]_D^{25} = 17.7$ (*c* 1, MeOH). HRMS (ESI⁺) calcd for C₅₁H₈₃N₉O₁₈S₃ ([M + 2H]²⁺): 602.7504, found 602.7506. ^1H NMR (DMSO) δ 0.82 (t, $^3J = 6.96$ Hz, 9H), 1.18–1.25 (m, 12H), 1.42 (m, 6H), 2.79 (t, $^3J = 7.24$ Hz, 6H), 3.19–3.26 (m, 3H), 3.34–3.45 (m, 9H), 3.66–3.78 (m, 6H), 4.62 (t, $^3J = 5.56$ Hz, 3H), 4.68 (s, 6H), 5.18 (2s, 9H), 5.31 (d, $^3J = 4.67$ Hz,

3H), 5.36 (d, $^3J = 6.03$ Hz, 3H), 5.53 (d, $^3J = 9.23$ Hz, 3H), 8.23 (s, 3H). ^{13}C NMR (DMSO) δ 14.3, 22.2, 29.2, 30.9, 38.2, 61.2, 64.2, 70.0, 71.8, 72.6, 77.4, 80.4, 87.9, 123.5, 140.4, 144.1, 147.3.

1,3,5-Tris[1-(β -D-glucopyranosyl)-1,2,3-triazole-4-yloxymethyl]-2,4,6-tris(hexylthio) benzene (**C6Glu3**)

Acetylated compound. Yield 643 mg (73%), white powder, R_f 0.47 in AcOEt/CH₂Cl₂ (4:6). Mp 123.7–125.4 °C. $[\alpha]_D^{25} = -54.8$ (*c* 1, CH₂Cl₂). ^1H NMR (CDCl₃) δ 0.87 (t, $^3J = 7.0$ Hz, 9H), 1.25–1.35 (m, 18H), (p, $^3J = 7.38$ Hz, 6H), 1.89 (s, 9H), 2.05–2.11 (3s, 27H), 2.79 (t, $^3J = 7.28$ Hz, 6H), 4.02 (m, 3H), 4.14 (dd, $^3J = 1.75$ Hz, $^2J = 12.53$ Hz, 3H), 4.3 (dd, $^3J = 4.96$ Hz, $^2J = 12.71$ Hz, 3H), 4.81 (s, 6H), 5.22–5.28 (m, 9H), 5.39–5.53 (m, 6H), 5.9 (d, $^3J = 8.85$ Hz, 3H), 7.83 (s, 3H). ^{13}C NMR (CDCl₃) δ 14.1, 20.2, 20.5, 20.6, 20.7, 22.5, 28.6, 29.6, 31.4, 38.9, 61.6, 64.2, 67.7, 70.2, 71.9, 72.8, 75.0, 85.7, 121.1, 141.1, 146.0, 147.0, 168.8, 169.4, 170.0, 170.5.

Deacetylated compound. Yield 347 mg (88%), white powder, R_f 0.46 in AcOEt/MeOH/H₂O (7:2:1). Mp 186.8–188.1 °C. $[\alpha]_D^{25} = -8.2$ (*c* 1, MeOH). HRMS (ESI⁺) calcd for C₅₄H₈₉N₉O₁₈S₃ ([M + 2H]²⁺): 623.7738, found 623.7739. ^1H NMR (DMSO) δ 0.82 (t, $^3J = 6.96$ Hz, 9H), 1.18–1.25 (m, 12H), 1.42 (m, 6H), 2.79 (t, $^3J = 7.24$ Hz, 6H), 3.19–3.26 (m, 3H), 3.34–3.45 (m, 9H), 3.66–3.78 (m, 6H), 4.62 (t, $^3J = 5.56$ Hz, 3H), 4.68 (s, 6H), 5.18 (2s, 9H), 5.31 (d, $^3J = 4.67$ Hz, 3H), 5.36 (d, $^3J = 6.03$ Hz, 3H), 5.53 (d, $^3J = 9.23$ Hz, 3H), 8.23 (s, 3H). ^{13}C NMR (DMSO) δ 14.3, 22.2, 29.2, 30.9, 38.2, 61.2, 64.2, 70.0, 71.8, 72.6, 77.4, 80.4, 87.9, 123.5, 140.4, 144.1, 147.3.

1,3,5-Tris[1-(β -D-glucopyranosyl)-1,2,3-triazole-4-yloxymethyl]-2,4,6-tris(heptylthio) benzene (**C7Glu3**)

Acetylated compound. Yield 645 mg (72%), white powder, R_f 0.54 in AcOEt/CH₂Cl₂ (4:6). Mp 134.2–136.7 °C. $[\alpha]_D^{25} = -50.8$ (*c* 1, CH₂Cl₂). ^1H NMR (CDCl₃) δ 0.88 (t, $^3J = 6.9$ Hz, 9H), 1.25 (m, 24H), 1.47 (p, $^3J = 7.54$ Hz, 3H), 1.89 (s, 9H), 2.05–2.11 (3s, 27H), 2.79 (t, $^3J = 7.3$ Hz, 6H), 4.02 (ddd, $^3J = 1.99$ Hz, $^3J = 5.27$ Hz, $^3J = 10.17$ Hz, 3H), 4.14 (dd, $^3J = 1.95$ Hz, $^2J = 12.54$ Hz, 3H), 4.3 (dd, $^3J = 4.97$ Hz, $^2J = 12.63$ Hz, 3H), 4.81 (s, 6H), 5.22–5.28 (m, 9H), 5.4–5.53 (m, 6H), 5.9 (d, $^3J = 8.98$ Hz, 3H), 7.83 (s, 3H). ^{13}C NMR (CDCl₃) δ 14.1, 20.2, 20.5, 20.6, 20.7, 22.6, 28.9, 29.7, 31.7, 38.9, 61.6, 64.2, 67.7, 70.2, 71.9, 72.8, 75.0, 85.7, 121.2, 141.1, 146.0, 147.0, 168.8, 169.4, 170.0, 170.5.

Deacetylated compound. Yield 341 mg (87%), white powder, R_f 0.53 in AcOEt/MeOH/H₂O (7:2:1). Mp 183.0–184.7 °C. $[\alpha]_D^{25} = -7.4$ (*c* 1, MeOH). HRMS (ESI⁺) calcd for C₅₇H₉₅N₉O₁₈S₃ ([M + 2H]²⁺): 644.7973, found 644.7978. ^1H NMR (DMSO) δ 0.85 (t, $^3J = 6.95$ Hz, 9H), 1.22–1.41 (m, 30H), 2.79 (t, $^3J = 6.77$ Hz, 6H), 3.17–3.27 (m, 3H), 3.36–3.45 (m, 9H), 3.67–3.76 (m, 6H), 4.62 (t, $^3J = 5.54$ Hz, 3H), 4.68 (s, 6H), 5.17 (2s, 9H), 5.3 (d, $^3J = 4.73$ Hz), 5.35 (d, $^3J = 6.06$ Hz, 3H), 5.53 (d, $^3J = 9.21$ Hz, 3H), 8.24 (s, 3H). ^{13}C NMR (DMSO) δ 14.4, 22.5, 28.7, 28.8, 29.6, 31.6, 38.3, 61.3, 64.2, 70.0, 71.7, 72.6, 77.4, 80.4, 87.9, 123.5, 140.3, 144.0, 147.2.

1,3,5-Tris(prop-2-ynyloxymethyl) benzene (4). To a solution of propargyl alcohol (311 mg, 5.5 mmol) in anhydrous DMF (8 mL) cooled to 0 °C, was added, little by little, under argon atmosphere a 60% NaH (131 mg, 5.5 mmol) oil dispersion. The reaction mixture was stirred for 10 min and a solution of tris(bromomethyl)benzene (505 mg, 1.4 mmol) in dry DMF (1 mL) was slowly added at 0 °C. The resulting mixture was stirred for 18 h at room temperature and ice was added to neutralize the basic solution. The mixture was poured into water (50 mL) and extracted with AcOEt (3 × 50 mL). The organic layers were gathered, washed first with H₂O (2 × 30 mL), then with brine (30 mL), dried with anhydrous MgSO₄, filtered and concentrated. Purification by flash chromatography on a silica gel column with CH₂Cl₂/cyclohexane (85:15) gave the expected product as yellow oil (511 mg, 48%). *R*_f 0.51 in CH₂Cl₂/cyclohexane (9:1). ¹H NMR (CDCl₃) δ 2.5 (t, ⁴*J* = 2.38 Hz, 3H), 4.22 (d, ⁴*J* = 2.38 Hz, 6H), 4.64 (s, 6H), 7.33 (s, 3H). ¹³C NMR (CDCl₃) δ 57.33, 71.30, 74.77, 79.55, 127.12, 137.93.

1,3,5-Tris[1-(β-D-glucopyranosyl)-1,2,3-triazole-4-yloxymethyl] benzene (C0Glu3). Compound C0Glu3 was obtained as described for the synthesis of C3Glu3 by using the appropriate 1,3,5-tris(prop-2-ynyloxymethyl)-benzene instead of 3a.

Acetylated compound. Yield 481 mg (50%), white powder, *R*_f 0.48 in AcOEt/CH₂Cl₂ (8:2). ¹H NMR (CDCl₃) δ 2.00–2.06 (3s, 26H), 4.04–4.32 (m, 9H), 4.55 (s, 6H) 4.62 (s, 6H), 5.27–5.88 (m, 9H), 6 (d, ³*J* = 9.04 Hz, 3H), 7.32 (s, 3H), 8.04 (s, 3H). ¹³C NMR (CDCl₃) δ 20.1, 20.5, 20.6, 20.7, 61.5, 62.7, 67.7, 70.3, 71.6, 72.7, 74.9, 85.6, 121.7, 127.3 138.2, 145.6 168.9, 169.5, 170.0, 170.5.

Deacetylated compound. Yield 308 mg (87%), white powder, *R*_f 0.51 in AcOEt/MeOH/H₂O (5:4:3). Mp 175.0–176 °C. [*α*]_D²⁵ = –7.4 (c 1, MeOH). ¹H NMR (DMSO) δ 2.51–3.47 (m, 24H), 3.68–3.82 (m, 6H), 4.15 (m, 3H), 4.57 (s, 6H), 4.60 (s, 6H), 4.68 (m, 3H), 5.24 (m, 3H), 5.39–5.46 (m, 9H), 5.54 (d, ³*J* = 9.2 Hz, 3H), 7.27 (s, 3H), 8.38 (s, 3H). ¹³C NMR (DMSO-*d*₆) δ 49.06, 61.20, 63.35, 69.99, 71.67, 72.51, 77.39, 80.40, 87.96, 123.82, 126.43, 138.77, 144.17.

Surface tension measurements

The surface activity of facial amphiphiles in solution at the air/water interface was determined by the Wilhelmy plate technique using a Krüss K100 tensiometer controlled by Labdesk software (Krüss, Germany). All solutions were prepared at least 12 hours before the measurements with water purified using a Milli-Q system (Millipore; resistivity = 18.2 MΩ cm; surface tension = 72.8 mN m⁻¹). A 20 mL initial volume of the facial amphiphile solution was taken in a glass trough, and surface tensions were determined by a dilution technique. The platinum plate was cleaned by flaming before experiments. All measurements were carried out at 25 °C and repeated 3 times unless otherwise noted. The surface excess *Γ* at the air–water interface was calculated by the Gibbs adsorption isotherm equation $\Gamma = -(1/RT)(d\gamma/d\log C)$, where γ is the surface tension (N m⁻¹) at the surfactant concentration *C* (mol L⁻¹). The occupied area (*A*_{min}) per surfactant molecule was calculated from $A_{\min} = 1/N_A\Gamma$, where *N*_A is Avogadro's number.

Dynamic light scattering measurements

Hydrodynamic diffusion coefficients and polydispersity index of CnGlu3 solutions at different concentrations were measured at 25 °C using a Zetasizer Nano-S model 1600 (Malvern Instruments Ltd., UK) equipped with a He–Ne laser ($\lambda = 633$ nm, 4.0 mW). The solutions were prepared and stored at room temperature overnight before measurements. The samples were filtered through a 0.45 μm filter and placed in a 45 μL-cuvette. The experimental run time was 10 s and experimental data are reported as an average of 10 values from 10 scans. Scattered light intensity was measured at a scattering angle of 173° relative to the laser source (backscattering detection). The time-dependent correlation function was analyzed using an exponential decay model. When there was a low polydispersity index (PDI < 20%), a Stokes radius (*R*_S) of particles was estimated from the diffusion coefficient (*D*) using the Stokes–Einstein equation $D = k_B T / 6\pi\eta R_S$, where *k*_B is the Boltzmann constant, *T* the absolute temperature and η the viscosity of the solvent. This enabled intensity size distribution to be converted into volume size distribution *via* the manufacturer's software, according to the Mie theory which gives a good estimation of the mean size of particles in solution.

Determination of log *k'**w* values

We used reversed-phase high-performance liquid chromatography, a common and rapid technique for indirect determination of the octanol/water partition coefficient as a measure of the lipophilicity of organic compounds. The facial amphiphiles were dissolved in MeOH at a concentration of 1 g L⁻¹ and injected into a reverse-phase column (C18, 5 μm granulometry, 250 × 4.6 mm) at room temperature.²⁵ Compounds were eluted with various MeOH/H₂O mixtures (from 95:5 to 65:35). The measurements were performed at a flow rate of 0.8 mL min⁻¹ and detected at 220 nm. The value of log *k'**w* was calculated as $\log k'w = \log[(t-t_0)/t_0]$, where *t* is the retention time of the compound and *t*₀ is the elution time of MeOH, which is not retained on the column. log *k'**w* values were obtained by extrapolation of the linear regression to 0% MeOH.

Small angle X-ray scattering (SAXS)

The structure of particles in solution (radius of gyration, dimensions of self-assembled structures, molecular mass) was characterized by SAXS using Synchrotron radiation on the ID14-eh3 beamline at European Synchrotron Research Facility (Grenoble, France). Scattering patterns were measured at several solute concentrations ranging from 2 to 40 g L⁻¹ in H₂O. For a sample–detector distance of 1.83 m and an X-ray wavelength $\lambda = 0.0931$ nm, a $0.01 < q < 3.5$ nm⁻¹ range of momentum transfer was covered. To avoid radiation damage during the scattering experiments, the sample was kept circulating in the cell while the data were collected in 10 successive 30 s frames. Individual frames were averaged after normalization to the intensity of the incident beam and corrected for detector response, and the scattering of the buffer was subtracted. The difference curves were scaled for the solute concentration. All data manipulations were performed *via* the program package PRIMUS.³⁴

The forward scattering values $I(q = 0)$ and the radii of gyration R_g were evaluated using the Guinier approximation assuming that, at very small angles ($qR_g < 1$), the intensity is represented as $I(q) = I(0)\exp(-qR_g^2/3)$. For rod-like particles, scattering curves were analyzed by plotting $qI(q) \approx \exp(-qR_g^2/2)$. The scattering data were separated into two parts: a low-angle range where the length of the rod $L = \sqrt{12} R_g$ can be determined and a higher-angle region where the diameter can be obtained from data at angles where $2\pi/L < q < 1/R_c$ (R_c is the cross-sectional radius of gyration). The molecular weight (MW) of the solutes was estimated by comparing their forward scattering intensity with that of a reference solution³⁵ of bovine serum albumin ($MW_{BSA} = 66$ kDa), corrected for electron density and partial specific volume of solutes. Partial specific volumes were estimated from the chemical compositions of the molecules. N_{agg} is calculated by dividing the aggregate molecular weight obtained from the forward intensity by the molecular weight of the monomer. The SAXS data in Fig. 7 were further analyzed using the SASfit software package.³⁶ For **C4Glu3** and **C5Glu3**, a model from Jan Skov Pedersen of rod-like copolymer micelles was used. This model worked reasonably well except for sample **C3Glu3**, which needed to be treated with a model of a generalized Gaussian coil.

Acknowledgements

We are grateful to the European Synchrotron Radiation Facility for provision of synchrotron radiation facilities and to Petra Pernot for assistance in using beamline ID14-eh3. We would like to thank Professor Marc Gingras for his helpful discussion concerning the synthesis of tripods, and Marjorie Sweetko for English language revision.

References

- (a) J. H. Fuhrhop and T. Wang, *Chem. Rev.*, 2004, **104**, 2901–2938; (b) F. M. Menger and J. S. Keiper, *Angew. Chem., Int. Ed.*, 2000, **39**, 1906–1920; (c) M. Wathier, A. Polidori, K. Ruiz, A.-S. Fabiano and B. Pucci, *New J. Chem.*, 2001, **25**, 1588–1599.
- Y. Zhao, *Curr. Opin. Colloid Interface Sci.*, 2007, **12**, 92–97.
- Y. Cheng, D. M. Ho, C. R. Gottlieb, D. Kahne and M. A. Bruck, *J. Am. Chem. Soc.*, 1992, **114**, 7319–7320.
- P. Venkatesan, Y. Cheng and J. D. Kahne, *J. Am. Chem. Soc.*, 1994, **116**, 6955–6956.
- Y. R. Vandenburg, B. D. Smith, M. N. Pérez-Payán and A. P. Davis, *J. Am. Chem. Soc.*, 2000, **122**, 3252–3253.
- U. Taotafa, D. B. McMullin, S. C. Lee, L. D. Hansen and P. B. Savage, *Org. Lett.*, 2000, **2**, 4117–4120.
- P. B. Savage, *Eur. J. Org. Chem.*, 2002, 759–768.
- H. M. Willemem, A. T. M. Marcelis and E. J. R. Sudhölter, *Langmuir*, 2003, **19**, 2588–2591.
- Z. Zhang, J. Yan and Y. Zhao, *Langmuir*, 2005, **21**, 6235–6239.
- (a) P. S. Chae, K. Gotfryd, J. Pacyna, L. J. W. Miercke, S. G. F. Rasmussen, R. A. Robbins, R. R. Rana, C. J. Loland, B. Kobilka, R. Stroud, B. Byrne, U. Gether and S. H. Gellman, *J. Am. Chem. Soc.*, 2010, **132**, 16750–16752; (b) D. T. McQuade, D. G. Barrett, J. M. Desper, R. K. Hayashi and S. H. Gellman, *J. Am. Chem. Soc.*, 1995, **117**, 4862–4869.
- F. M. Menger and J. L. Sorrels, *J. Am. Chem. Soc.*, 2006, **128**, 4960–4961.
- J. A. A. W. Hlemons, R. R. J. Slangen, A. E. Rowan and R. J. M. Nolte, *J. Org. Chem.*, 2003, **68**, 9040–9049.
- R. Roy and J. M. Kim, *Angew. Chem., Int. Ed.*, 1999, **38**, 369–372.
- M. Kellermann, W. Bauer, A. Hirsch, B. Schade, K. Ludwig and C. Böttcher, *Angew. Chem., Int. Ed.*, 2004, **43**, 2959–2962.
- (a) S. Jebors, F. Fache, S. Balme, F. Devoge, M. Monachino, S. Cecillon and A. W. Coleman, *Org. Biomol. Chem.*, 2008, **6**, 319–329; (b) K. Suwinska, O. Shkurenko, C. Mbemba, A. Leydier, S. Jebors, A. W. Coleman, R. Matar and P. Falson, *New J. Chem.*, 2008, **32**, 1988–1998.
- A. P. H. J. Schenning, C. Elissen-Romàn, J.-W. Weener, M. W. P. L. Baars, S. J. van der Gaasdt and E. W. Meijer, *J. Am. Chem. Soc.*, 1998, **120**, 8199–8208.
- K. Ariga, T. Urakawa, A. Michiue, Y. Sasaki and J.-I. Kikuchi, *Langmuir*, 2000, **16**, 9147–9150.
- Y. Chen, A. V. Ambade, D. R. Vutukuri and S. Thayumanavan, *J. Am. Chem. Soc.*, 2006, **128**, 14760–14761.
- K. V. Kilway and J. S. Siegel, *Tetrahedron*, 2001, **57**, 3615–3627.
- J. E. Anthony, S. I. Khan and Y. Rubin, *Tetrahedron Lett.*, 1997, **38**, 3499–3627.
- M. Gingras, J.-M. Raimundo and Y. M. Chabre, *Angew. Chem., Int. Ed.*, 2006, **45**, 1686–1712.
- (a) H. C. Kolb, M. G. Finn and K. B. Sharpless, *Angew. Chem., Int. Ed.*, 2001, **40**, 2004–2021; (b) V. V. Rostovtsev, L. G. Green, V. V. Fokin and K. B. Sharpless, *Angew. Chem., Int. Ed.*, 2002, **41**, 2596–2599.
- F. Fazio, M. C. Bryan, O. Blixt, J. C. Paulson and C. H. Wong, *J. Am. Chem. Soc.*, 2002, **124**, 14397–14402.
- C. Tanford, in *The hydrophobic effect: formation of micelles and biological membranes*, Krieger publishing company, Malabar Florida, 2nd edn, 1991.
- T. Braumann, *J. Chromatogr., A*, 2008, **373**, 191–225.
- D. Svergun, *J. Appl. Crystallogr.*, 1992, **25**, 495–503.
- R. Pecora, Basic Concepts Scattering and Time Correlation Functions, in *Soft Matter Characterization*, ed. Borsali and Percora, Springer, 2007, vol. 1, pp. 1–38.
- (a) C. Tanford, *J. Phys. Chem.*, 1972, **76**, 3020–3024; (b) Israelachvili, D. J. Mitchell and B. W. Ninham, *J. Chem. Soc., Faraday Trans. 2*, 1976, **72**, 1525–1568; (c) K. Kratzat and H. Finkelmann, *Langmuir*, 1996, **12**, 1765–1770.
- R. Ngarajan, *Langmuir*, 2002, **18**, 31–38.
- B. Trappmann, K. Ludwig, M. R. Radowski, A. Shukla, A. Mohr, H. Rehage, C. Böttcher and R. Haag, *J. Am. Chem. Soc.*, 2010, **132**, 11119–11124.
- K. Kratzat and H. Finkelmann, *J. Colloid Interface Sci.*, 1996, **181**, 542–550.
- P. Garidel, A. Hildebrand, R. Neubert and A. Blume, *Langmuir*, 2000, **16**, 5267–5275.
- A. Hidebrand, P. Garidel, R. Neubert and A. Blume, *Langmuir*, 2004, **20**, 320–328.
- P. V. V. Konarev, V. Vladimirov, A. V. Sokolova, M. H. J. Koch and D. Svergun, *J. Appl. Crystallogr.*, 2003, **36**, 1277–1282.
- E. Mylonas and D. I. Svergun, *J. Appl. Crystallogr.*, 2007, **40**, s245–s249.
- J. Kohlbrecher, SASfit ver. 0.93.3; available at <http://kur.web.psi.ch/sans1/SANSSoft/sasfit.html>.